iMag+: An Accurate and Rapidly Deployable Inertial Magneto-Inductive SLAM System

Bo Wei, Niki Trigoni, *Member, IEEE,* Andrew Markham

***Abstract*—Localisation is an important part of many applications. Our motivating scenarios are short-term construction work and emergency rescue. These scenarios also require rapid setup and robustness to environmental conditions additional to localisation accuracy. These requirements preclude the use of many traditional high-performance methods, e.g. vision-based, laser-based, Ultra-wide band (UWB) and Global Positioning System (GPS)-based localisation systems. To overcome these challenges, we introduce *iMag+*, an accurate and rapidly deployable inertial magneto-inductive (MI) mapping and localisation system, which only requires monitored workers to carry a single MI transmitter and an inertial measurement unit in order to localise themselves with minimal setup effort. However, one major challenge is to use distorted and ambiguous MI location estimates for localisation. To solve this challenge, we propose a novel method to use MI devices for *sensing environmental distortions* for accurate closing inertial loops. We also suggest a robust and efficient first quadrant estimator to sanitise the ambiguous MI estimates. By applying robust simultaneous localisation and mapping (SLAM), our proposed localisation method achieves excellent tracking accuracy and can improve performance significantly compared with only using a Magneto-inductive device or inertial measurement unit (IMU) for localisation.**

***Index Terms*—Magneto-inductive device; Inertial measurements; Localisation; SLAM**

I. Introduction

This paper proposes iMag+, an accurate, robust and rapidly deployable Simultaneous Localisation and Mapping (SLAM) system. We aim to estimate the location of monitored people in challenging environments, i.e. areas where traditional wireless radio or vision based systems fail or are not sufficiently robust. Personal localisation systems have a broad range of applications, such as emergency response [1], indoor location-based service [2], [3] or construction site safety [4]. iMag+ uses inertial measurements for pedestrian dead reckoning and Magneto-Inductive (MI) measurements for loop closure and correcting accumulated drift from inertial sensors. A key feature of our proposed method is the ability to deploy a single transmitter in the area of interest and immediately start tracking. This is in stark contrast to other approaches, e.g. Ultra-wideband (UWB), which need a large number of non-colocated anchors to be surveyed in place.

Motivating Scenario: short-term construction work. Official government reports indicate that workforce fatalities or injuries to railway workers often occur due to insufficient warnings when plant machinery or a train approaches [5], [6]. Here is an example scenario. Ten workers arrive at a railway construction site within a tunnel at 8:00 am. A localisation system needs to be set up to warn workers when they enter a static danger zone or when their working area becomes a danger zone due to an oncoming train. The plan is to commence work by 8:15 am, after a short site inspection. Many localisation techniques can achieve sub-metre accuracy, such as those using Global Positioning System (GPS) [7] , laser [8], camera [9] or UWB [10]. However, these techniques either require extensive site surveys and map-construction (e.g. UWB, camera, laser) or do not work well within enclosed areas like tunnels (e.g. GPS). The traditional method of ensuring track-worker safety is mainly manual, through protection officers acting as a look-out and using the Autoprowa warning system [11], i.e. a light and horn, to warn construction workers. This needs additional labour, and more importantly, lookouts need to be alert for an entire shift. Furthermore, bad weather like fog and rain also severely affects the lookout range of protection officers. GPS is also popular for outdoor localisation applications [12], [13], [14], but its positioning is only relatively accurate in a very clear sky view. UWB is a promising technology for localisation with centimetre-level accuracy, but it is time-consuming to deploy infrastructure. The basic principle behind UWB localisation is a trilateration method using estimated distances from receivers to transmitters. In other words, it requires multiple transmitters deployed in the area (at least three transmitters for 2D localisation or four transmitters for 3D localisation). In short-term construction work, it is time-consuming and tedious to install and configure a UWB localisation system. Obstacles, such as vegetation and machinery, can also easily attenuate UWB signals, limiting their use in our motivating scenarios. Many SLAM systems also fuse various types of measurements. Among them, camera-inertial and laser-inertial methods are popular and able to attain superior performance. However, both of them still have

Fig. 1. Motivating scenario: short-term construction work (a) near a rail track (b) on road.

Bo Wei is with the Department of Computer and Information Sciences at Northumbria University, UK, e-mail: bo.wei@northumbria.ac.uk (Bo Wei is the corresponding author).

Niki Trigoni is with the Department of Computer Science at Oxford University, UK, e-mail: niki.trigoni@cs.ox.ac.uk.

Andrew Markham is with the Department of Computer Science at Oxford University, UK, e-mail: andrew.markham@cs.ox.ac.uk.

drawbacks. Bad weather (e.g. fog, rain and snow), low visual texture/features in the surrounding environment (e.g. dust and muddy ground) and poor lighting condition contrive to impact even the most sophisticated vision-based localisation methods. Furthermore, dynamic environments, e.g. moving workers, can create difficulties for laser-based applications.

Magneto-Induction (MI) uses very low frequency (e.g. 2.5 kHz) fields that are generated at a transmitter. They have many key advantages over electromagnetic (Radio frequency (RF), vision, laser) based techniques in that they allow through-obstacle localisation without requiring a line-of-sight connection [15]. In addition, as we use a triaxial transmitter and receiver, only a pair of devices is required to determine 3-D position and orientation. However, MI localisation systems are still *challenging* due to their difficulties in obtaining an accurate localisation estimate, especially at longer ranges. One localisation system [16] has been proposed based on MI and inertial measurements, and it uses a particle filter for data fusion. However, it requires determining environmental specific parameters, i.e. time-consuming configuration for *each* MI transmitter/receiver pair and *each* specific environment. It is infeasible to exploit this method for rapidly deployable localisation. In our previous paper [17], we propose an alternative method iMag for using MI devices for localisation. In our proposed method, we no longer conduct environmental surveying. Instead, we leverage MI devices to sense environmental distortions and create unique spatially linked signatures. These unique spatial features are used for loop closure and calibrating biased pedestrian navigation trajectories derived from inertial measurements. To further improve the localisation performance, we propose an innovative iMag+ SLAM system in this paper, which applies an efficient first quadrant estimator to sanitise the ambiguous MI estimates. A robust SLAM framework is also employed in order to improve localisation accuracy.

To summarise, the contributions of this paper are:

- We first propose an innovative method to enable MI devices to sense environmentally induced distortions. Spatial signatures are created by MI measurements to enable minimal effort for configuring MI devices. We take advantage of these features for loop closure and calibrating biased navigation trajectories.
- We study the performance of MI estimates in typical outdoor and indoor environments, and demonstrate that MI measurements are highly jeopardised by ambiguity issues and distortion. We propose an efficient first quadrant estimator to mitigate severe MI ambiguity issues, which is further used for data fusion.
- We propose the iMag+ SLAM system, which performs data fusion using MI and inertial measurements to achieve robust localisation with high accuracy.
- A prototype SLAM system has been implemented. Only one MI transmitter is deployed in the area of interest, which enables the rapid setup. Extensive experiments are performed at our campus and in one multi-storey building to evaluate our proposed method and show the advantage of the MI signal compared with other wireless signals for localisation.

The rest of this paper is organised as follows. Related work is demonstrated in Section II. Section III presents the system overview of our proposed localisation method. Section IV shows the details of the method using MI and inertial measurements for sensing environments and localisation. Evaluations are shown in Section V. Finally, we conclude this paper and present the future work in Section VI.

II. Related Work

In this section, we outline related research in three main areas: MI applications, high-resolution sensor based localisation, and wireless signal based localisation methods.

A. Magneto-Inductive Localisation and Communication

Recently, a number of MI-based devices have been designed for localisation. [18] designs a magnetic device for proximity detection for indoor applications. [19] uses MI-based signal to monitor the locations of underground animals. As the magnetic signal can penetrate soil and water, it achieves good accuracy and outperforms all other existing methods. [20], [21] obtain an MI-based range estimate first and then uses multilateration to estimate the location of monitored people.

We are not the first to consider fusing inertial measurements with MI. [16] implements a 3-D inertial-MI system and performs data fusion using a simple particle filter model. They use inertial measurements along with the absolute positioning from the MI signal, which needs careful calibration for each receiver-transmitter pair. On the contrary, our method takes advantage of unique spatial features, so there is no need to have prior knowledge of a device and its operating environment.

Benefitting from the absence of multipath effect and the perpetration of a non-metal material, MI-based devices are also designed for communication in extreme environments. [22], [23], [24], [25] propose to use MI devices for communication undersea, underground and in district heating system, respectively.

B. High-resolution Sensor based Localisation Methods

There are many localisation systems based on high-resolution sensors, e.g. camera [9] and laser [8]. They can achieve centimetre accuracy in ideal conditions, but they have some key disadvantages that make them not particularly well suited to our motivating application scenario. Camera-based localisation is extremely sensitive to poor lighting conditions, occlusions and dust. Similarly, laser-based localisation is costly and can struggle with highly dynamic environments. Our motivating application scenario is short term construction work with a poor lighting condition and a dynamic surrounding environment, which makes our proposed MI-based solution a better candidate for the application scenario.

C. Wireless Signal Based Localisation Methods

WiFi signals are widely available in office and residential environments, and as a result, many solutions have been proposed for fusing WiFi and inertial measurements, such as [26], [27], [28]. However, WiFi is highly affected by

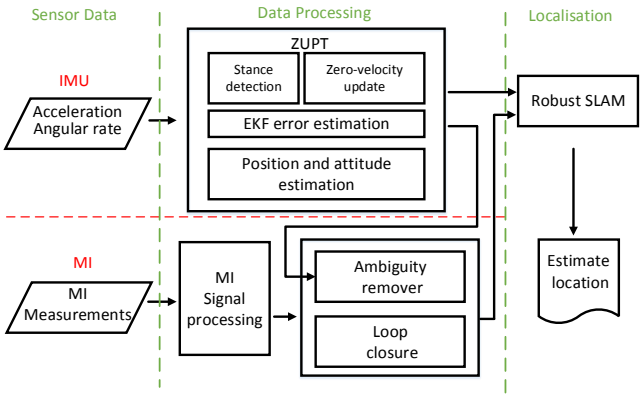

Fig. 2. System Flow Chart

multipath and would require a number of transmitters to be installed in the operating area. In addition, the accuracy of WiFi-based systems is typically in the 3-5 m region, due to variance in RSSI measurements and sensitivity to orientation and obstacles.

As an alternative spatially varying signal, the earth's magnetic field has been explored as a positioning modality. This is because it is influenced by ferrous objects in the surrounding environment, such as reinforcing steel inside buildings that distorts the earth's magnetic field. [29], [30], [31], [32], [33] combine these spatial features and inertial measurements for positioning. However, it is difficult to exploit these signatures in an outdoor environment, where motion is less constrained, and the spatial signatures are less informative due to a lack of metal.

UWB is an emerging state-of-the-art localisation infrastructure. It can achieve centimetre-level accuracy. With inertial measurements, it can track activity and gesture as well as localisation [34]. UWB does require a good transmitter geometry to be installed in the operating area and have a good line-of-sight. Furthermore, the weak UWB signals are easily blocked by obstacles and vegetation, which impacts its robustness.

III. System Overview

To address the key challenges faced by teams of construction workers, the proposed system must satisfy the following three requirements:

- Localisation accuracy: workers must be positioned with metre level accuracy in any environment.
- Robustness: the system must be immune to non-line-of sight conditions and changes in the operating environment.
- Rapid deployment: the system must be easy to initialise to ensure compliance and adoption through low operator effort.

A system flow chart of our proposed localisation method is shown in Figure 2. Inertial measurements (i.e. acceleration and angular rate measurements) and MI measurements are first collected. Acceleration and angular rate measurements come from a foot-mounted inertial measurement unit (IMU). A standard zero velocity update (ZUPT) [35] based tracker generates an inertial trajectory subject to accumulative drift.

A single MI transmitter is placed in the Area of Interest, with each worker wearing a small MI receiver. The received MI signals are first cross-correlated with a reference template to extract the channel matrix. From the channel matrix and a standard physical model, a user's position is estimated. Note, however, that this is typically incorrect due to distortions in the MI field. Furthermore, due to the long integration time (approximately 1 second in this case), user motion induces random quadrant ambiguities, i.e. x and y co-ordinates can be rotated by multiples of 90 degrees. It is clearly impossible to move from one side of the transmitter to the other in the matter of a second because of the dynamics of human motion, and thus these are first corrected with our suggested coordinate ambiguity removal method. This distorted trajectory is metrically compromised, but temporally stable and thus can serve as an indicator of loop closure. The loop closures from MI and the drifting inertial odometry are then passed into a Robust SLAM estimator to determine an accurate trajectory.

To summarise, the algorithmetic contributions in this paper are (R1) an effective methods for obtaining high-quality loop closure constraints (described in Sections IV-A and IV-B) and (R2) an efficient method for closing loops using MI measurements (described in Section IV-C). The main challenges for the research question (R1) are that of the localisation failure due to distorted MI and its impaired measurements in complex indoor environments due to ferrous influence. The research question (R2) also faces the challenge of a heavy computational burden.

IV. Inertial Magneto-Inductive Localisation

In this section, we present the details of our proposed inertial magneto-inductive SLAM system, iMag+.

A SLAM system aims to achieve an optimal trajectory J^* for the following formula,

$$\underset{J}{\operatorname{argmin}} \sum_{i \in C(J)} u_i^T \Theta_i u_i \tag{1}$$

where J is the estimated trajectory, $C(J)$ is the constraint set including motion and loop closure constraints, u and Θ are relevant error terms and information matrix[1]. In our system, the SLAM optimiser considers constraints from two sources, motion constraints from the IMU trajectory and loop closures from MI devices.

iMag+ uses a foot-mounted IMU to derive an trajectory, processed by the ZUPT algorithm. Overall, the performance of the foot-mounted inertial navigation is generally good, but due to sensor noise and bias, the trajectory will inevitably slowly drift over time.

To overcome this accumulative drift, iMag+ uses spatially unique features from MI measurements to detect loop closures and hence correct long-term errors in inertial odometry. An MI transmitter consists of three orthogonal coils which are tuned to resonance and driven with a coded binary phase shift keying (BPSK) message. This code is chosen to have desirable cross-correlation properties to increase the range of detectability.

[1]More details about SLAM can be found in [36], [37], [38]

The MI receiver similarly consists of three orthogonal sensors (again coils in our case), which are connected to low noise amplifiers and a wide dynamic range ADC. The wide dynamic range is necessary to handle the high path-loss exponent due to the near-field coupling - the field roll-off is 60 dB/decade, rather than the more typically encountered 40 dB/decade for electromagnetic propagation. The triaxial signals are then cross-correlated with the template code in order to estimate the channel matrix.

Once we have the channel estimates, we use the theory in [15], [16] to obtain 3-D position estimates[2]. Note, however, that these position estimates are distorted by nearby ferrous objects. The distortions mainly cause arbitrary rotations of the position estimates. However, we note that these distortions are constant over time, i.e. if the same point is revisited, then the same distorted position estimate will be obtained. It is this property that we aim to exploit to close loops and provide accurate long-term tracking.

However, before we use MI estimates for localisation or sensing environment, three issues have to be addressed: *(1) location distortion, (2) coordinate ambiguity, and (3) MI data association failure*. These arise mainly because of environmental noise, the motion of the user, and the configuration of the MI system. Previous research [16] requires labour-expensive calibration of MI transmitter-receiver pairs to solve these issues for each environment. Rather than explicit calibration, we are the first to study the feasibility of exploiting these distortions to indirectly sense the operating environment and create spatially linked MI features.

We conduct an outdoor experiment to demonstrate the issues faced by MI observations. We put one MI transmitter about 10 m away from the MI receiver, with a ground truth location of $(5.5, 9.1)$, as shown in Figure 3(a). Using the data processing described in [16], we find MI estimates are ambiguous, i.e. locations are estimated in different quadrants (shown in Figure 3(b)) instead of one.

Our previous research [17] proposed a coordinate ambiguity remover to sanitise the MI estimates, which gauges the current MI estimate based on the previous one and the user motion. This mechanism helps remove the coordinate ambiguity and improve the efficacy of loop closure. However, this will raise issues when the system is used in one indoor environment. Complex indoor environments with ferrous objects can result in the reduction of the sensing range. The packet loss caused by the range reduction introduces long-term intervals between two MI estimates. When using the coordinate ambiguity remover, the long-term intervals introduce errors, resulting in additional false negatives for loop closure. Therefore, we extend the localisation architecture and propose a simple technique to remove quadrant ambiguity, as detailed below, to improve its efficiency and the localisation performance.

A. Coordinate Ambiguity Removal: First Quadrant Estimator

One issue for the application of MI measurements is a quadrant coordinate ambiguity as shown in Figure 3(b). Theoretically, MI measurements should only be impacted by a hemispherical ambiguity. However, due to noise impacting the channel matrix pseudo-inverse, MI devices may still create ambiguous observations, especially when the height above ground is small. These quadrant ambiguities manifest as flips across the x-axis or/and y-axis.

Instead of trying to estimate the quadrant of each MI location as previously used in our previously proposed iMag [17], we assume they are all located in one quadrant (the first quadrant in our case). Specifically, the initial i-th MI estimate is $m_i = (x_i, y_i)$, so the sanitised i-th MI estimate is $\hat{m}_i = (|x_i|, |y_i|)$. We denote this method as First Quadrant Estimator. Please note, the mechanism will bring a large number of false positives for loop closure, and this will be resolved by using the robust SLAM optimiser which will be later introduced in the section.

B. Exploiting Distorted Locations

Instead of trying to overcome distortions and restore absolute MI positions, we simply accept that MI locations are not directly related to real-world coordinates through a pre-defined physical model. We consider sanitised MI estimates as observations in specific positions, termed as "*MI observations*", i.e. spatial features.

However, this perspective also indicates another important fact, i.e. *even though MI estimates cannot determine the correct global locations, they are unique to a specific location.* In other words, they have good discriminative power to indicate when a monitored person returns to the same point. Therefore, a single MI transmitter-receiver pair along with motion updates from inertial measurements can be used for accurate localisation, meeting the requirements of rapid deployment.

C. Loop-closure Extraction

When a monitored person re-enters a known area, the current spatial features match previous ones stored in a map. The repeated MI observations can close an estimated trajectory loop and adjust the biased inertial trajectory.

Our MI devices have an update rate of approximately 1.4 Hz, which means it can obtain an estimate every approximately 0.7 second. The disadvantage of low sampling rate is two-fold. Firstly, the device rotation over this period can result in an incorrect MI channel estimation, due to the signal smearing between the axes, corrupting the channel matrix. Secondly, the collection density of the MI spatial features is low, i.e. we have sparse features to use as loop-closure key points. However, we note that the MI distortions lie on a smooth surface, i.e. it is only large ferrous objects in the environment that can distort the MI field. The resultant field is an additive contribution from the MI source and the distorters.

Due to the smoothness of the location distortions, MI estimates can be interpolated by a linear model. A simple approach would be to upsample MI measurements into a denser grid, which would allow for more frequent loop-closure detection, as shown in Figure 5(a). Since the MI estimation rate is lower than inertial measurements, we can conduct linear

[2]The magnetic dipole equations are introduced in [15] and applied in [16] for 3-D localisation.

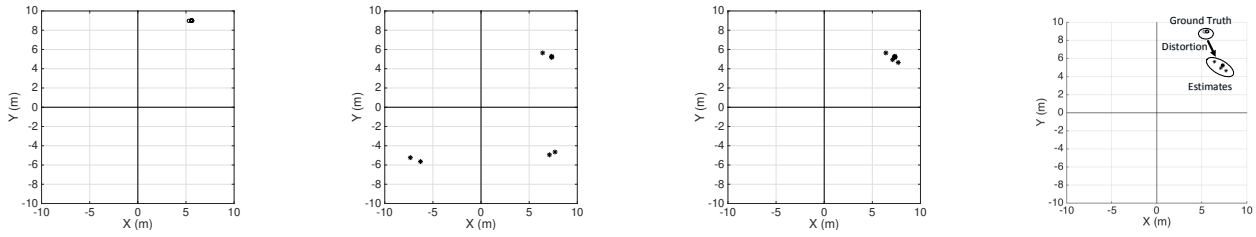

(a) (b) (c) (d)

Fig. 3. Experiment results showing MI issues (a) Ground truth. (b) Original MI estimates. (c) Optimised MI estimates using ambiguity remover (d) MI estimates showing distortion from ground-truth

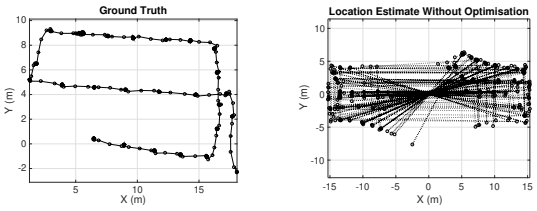

(a) (b)

Fig. 4. Performance of MI ambiguity remover (a) Ground truth (b) Original MI estimates.

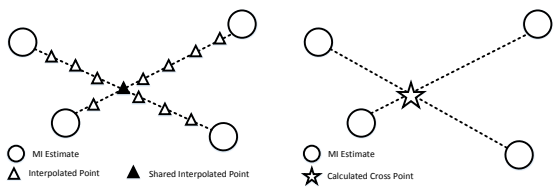

(a) (b)

Fig. 5. (a) Loop closure using interpolation method. (b) Loop closure using cross-point method

interpolation for MI estimation, using the inertial measurement interval to distribute the points. A Euclidean distance threshold can be set to determine whether two points are in the same location or not, to detect potential loop-closures.

However, we propose a more computationally efficient method, which detects intersections of two line segments whose endpoints are neighbouring MI estimates, and we call this "cross-point" method. We use a curve intersection detection method in [39], as shown in Figure 5(b) .

Here we present the details of this method. We have two line segments M_i and M_j (obtained from inertial trajectories) with end points which are neighbouring MI estimates. The end points of M_i and M_j are $(m_i(1), m_i(2))$, $(m_{i+1}(1), m_{i+1}(2))$ and $(m_j(1), m_j(2))$, $(m_{j+1}(1), m_{j+1}(2))$, respectively. There are four unknowns here $d1$, $d2$, x_0 and y_0. (x_0, y_0) is the intersection point. $d1$ and $d2$ are the distance between starting points and intersection points relative to the length of two segments. The relation among these variables are shown in the simultaneous equations in Equation (2).

$$\begin{cases} (m_{i+1}(1) - m_i(1)) \times d1 = x_0 - m_i(1) \\ (m_{i+1}(2) - m_i(2)) \times d1 = y_0 - m_i(2) \\ (m_{j+1}(1) - m_j(1)) \times d2 = x_0 - m_j(1) \\ (m_{j+1}(2) - m_j(2)) \times d2 = y_0 - m_j(2) \end{cases} \tag{2}$$

In matrix form, we have $A \times U = B$, where A, U and B are shown in Equation (3), Equation (4) and Equation (5). U is the unknown matrix, and can be solved by $U = B \setminus A$.

$$A = \begin{bmatrix} m_{i+1}(1) - m_i(1) & 0 & -1 & 0 \\ 0 & m_{i+1}(2) - m_i(2) & -1 & 0 \\ m_{j+1}(1) - m_j(1) & 0 & 0 & -1 \\ 0 & m_{j+1}(2) - m_j(2) & 0 & -1 \end{bmatrix} \tag{3}$$

$$U = \begin{bmatrix} d1 & d2 & x_0 & y_0 \end{bmatrix}^T \tag{4}$$

$$B = \begin{bmatrix} -m_i(1) & -m_i(2) & -m_j(1) & -m_j(2) \end{bmatrix}^T \tag{5}$$

After solving the equation, we need to check $d1$ and $d2$ to find if these two line segments have an intersection or not. If both $d1$ and $d2$ are between 0 and 1, it means these two line segments intersect, and (x_0, y_0) is the intersection point.

We denote s_{imu} and s_{mi} as the sampling rate of the motion sensor and the MI device, respectively. The sampling rate of the motion sensor is greater than that of MI devices, so $s_{imu} = k s_{mi}$, where $k > 1$. The number of samples are computed as $n_j = s_j \times t, j \in \{imu, mi\}$, where t is the data collection duration. The computation complexity of the linear interpolation and cross-point methods are both $O(n^2)$. However, the number of samples n used by the linear interpolation method is n_{imu}, while that used by the cross-point method is n_{mi}. In other words, the calculation complexity decreases by a scale factor of $1/k^2$ when using the cross-point method, which makes it approximately an order of magnitude faster than dense interpolation. This is of key importance for a real-time localisation system, especially when a large number of candidate loop-closure points are being searched and k is large[3].

[3]Using our devices shown in Section V, k is approximately 70.

D. Robust Map Building

Even with the use of state-of-the-art MI devices and our proposed method, it is still difficult to have perfect outlier-free loop closures. Therefore, our proposed system uses a robust GraphSLAM optimiser [40], [38]. The original GraphSLAM optimiser [41] considers all the constraints from odometry and loop closures with equal weights, as shown in Equation 1. On the contrary, in the robust map optimiser, the optimal trajectory J^* will be derived using the following optimiser instead [38],

$$\underset{J}{\operatorname{argmin}} \underbrace{\sum_{i \in O(J)} u_i^T \Theta_i u_i}_{\text{P1: Odometry constraints}} + \underbrace{\sum_{i \in L(J)} w_i^2 u_i^T \Theta_i u_i}_{\text{P2: Loop closure constraints}} \quad (6)$$

Note that the robust optimiser considers two joint parts, i.e. P1 and P2, for optimisation from odometry constraints $O(J)$ and loop closure constraints $L(J)$, respectively. Similar as Equation 1, u and Θ are the error terms and information matrix in Equation 6. Scaling factors w_i for information matrices are added to the loop closure constraints to increase robustness to outliers. The scaling factors w can be calculated using the following equation[4]:

$$w_i = \min(1, 2\Upsilon/(\Upsilon + E_i^2)) \quad (7)$$

where Υ is a free parameter and $E = u_i^T \Theta_i u_i$ in P2 from Equation 6. The use of the scaling factors w can effectively reduce the impact of false positive loop closures. With the new coordinate ambiguity removal method, many false positive loop closures will be detected. This issue can be handled by the robust GraphSLAM optimiser by calibrating scaling factors w and increasing the confidence of inertial measurements (P1) during the optimisation.

V. Evaluation

In this section, to show the advantage of MI measurements for indoor localisation, we firstly conduct experiments to compare the performance of MI measurements with that of WiFi and UWB in the lab (Experiment 1). We further evaluate the performance of our proposed iMag+ in both an outdoor environment with little vegetation (Experiments 2 and 3 shown in Figure 6(a)) and a multi-storey indoor environment (Experiment 4).

All of the experimental areas are a 40 m $\times$ 40 m space. We use the RTK GPS [7] and Tango [42] to record ground truth when conducting experiments at our campus and the building, respectively. RTK GPS and Tango can achieve good precision for their usage environment but fail to work in the opposite environment. The RTK GPS requires a clear sky view in an outdoor environment to obtain the signal for its usage, and Tango fails to work in the outdoor environment with few exploitable visual features. These facts also confirm the advantage of our proposed system as it is capable of being readily employed in both outdoor and indoor environments. The goal of our experiments 2-4 is to localise the monitored person and evaluate the accuracy of our proposed methods. We compare our proposed *iMag+* with localisation methods only using *IMU* and *MI* as well as our previous proposed iMag localisation method [17]. [5].

[4]The detailed derivation process and analysis can be found in [38]

(a) Campus

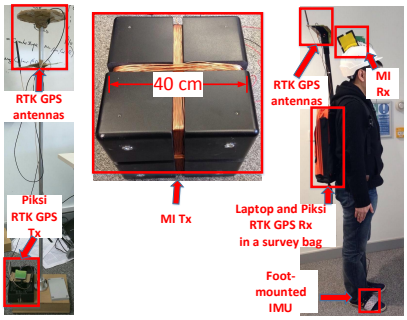

(b) Hardware (Tx and Rx are short for transmitter and receiver respectively)

Fig. 6. Experimental Setup

The following metrics are used in the experiments 2-4: (1) *Cumulative distribution function (CDF)*: The CDF of an error is a function whose value is the possibility that a corresponding estimate is less than or equal to the argument of that error; (2) *Root Mean Square Error (RMSE)*: (e_{rms}) is the mean localisation error over the entire trajectory, defined as $e_{rms} = \sqrt{\frac{1}{t_e - t_s} \Sigma_{t=t_s}^{t_e} \hat{e}(t)^2}$. $\hat{e}(t)$ is the localisation error for time t, expressed as $\hat{e}(t) = \|\hat{l}(t) - l_g(t)\|$, where $\hat{l}(t)$ and $l_g(t)$ are estimates and ground truth, respectively. CDF of standard deviations is also used in experiment 1 to show the signal variety level and compare the performances among MI, UWB and WiFi in terms of spatial features.

A. Hardware for Localisation

In this section, we describe the hardware we use for experiments. Our prototype includes a laptop, an MI transmitter, an MI receiver and an IMU as shown in Figure 6(b). An RTK GPS is used for recording ground truth in the outdoor environment, which can achieve 10 cm accuracy with a clear sky view. In the indoor environment without RTK GPS signal, we exploit visual odometry based Tango to record groundtruth[6]. In our prototype, a laptop is carried by the monitored person to collect and process measurements. It has an Intel Core i7

[5]The localisation results only using MI are from our previous research work [17] that sanitises the MI measurements and derives an MI-only trajectory.

[6]The long-term localisation shift still exists when using Tango, and we close loops manually to obtain good quality ground truth.

with 2.8 GHz processor and 16 GB Memory. The operating system is Ubuntu 14.04.

The MI transmitter includes a 40 cm plastic cube former which has three mutually orthogonal coils. Each coil is 25 turns of 1 mm diameter enamelled copper wire. Powered by a 1.2 Ah 12 V battery, three H-bridges amplify the modulated BPSK signals generated by an STM32F4 microcontroller. The message is modulated at a rate of 31.25 bps. The transmitter operates at a nominal centre frequency of 2.5 kHz. Similar to the MI transmitter, the MI receiver consists of a 10 cm plastic cube former wrapped by three mutually orthogonal coils of 150 turns/0.5 mm diameter enamelled copper wire. An ADS1274I 24 bit ADC is used for digitising received signals that are amplified by a transimpedance LNA. An STM32F4 micro-controller then processes the digital signals, dropping them down to baseband and performing carrier wiping and phase recovery. A USB cable is used to connect the MI receiver to the laptop in order to transfer collected data and power the MI receiver.

The IMU we employ is the development board Xsens MTi-3-8A7G6-DK [43]. In our system, it continuously supplies inertial measurements, i.e. acceleration and angular rate, both at 100 Hz. The IMU is firmly mounted on one foot of a monitored person, and the inertial measurements are ported to the laptop through a USB cable for further processing.

B. Experiment 1: Comparison with WiFi and UWB

In this experiment, we compare the stability and robustness of MI signals with WiFi and UWB in various scenarios. A wireless signal's temporal stability and robustness to environmental changes play an essential role in robust loop closure using the similarity of signals' spatial features. WiFi and UWB are two types of popular wireless signals for indoor localisation[27], [26], [28], [31], [10].

Due to the different units of each signal, we calculate the standard deviations of measurements for each type of signal in this experiment and show them in a standardised CDF. The origin of the CDF is the mean for each signal. We placed the MI, WiFi and UWB transmitters of MI, WiFi and UWB in close proximity to one another (within 10 cm) so that they have the same surrounding environment. We use a pair of UWB transceivers from Decawave TREK1000 evaluation kit [44]. One of the UWB transceivers acts as the transmitter, and the other one is the receiver. In terms the WiFi setup, we use one WiFi router as the transmitter and one laptop as the receiver. The measurements for MI for this experiment are MI observations, and the measurements for WiFi and UWB are RSS values and the distance measurements respectively. In this experiment, we will show the advantages of MI observations as unique spatial features in the following four scenarios.

Experiment 1(a) Temporal Stability: It is a prerequisite that wireless signal measurements are relatively constant when revisiting the same location after a certain period. Therefore, firstly, we evaluate the temporal stability of MI, WiFi and UWB measurements, respectively. We placed MI, WiFi and UWB receivers in one location, which is 2 m away from their transmitters. Figure 7(a) shows the CDF of standard deviations. Almost 100% of all the measurements from these three types of signals are within 3 standard deviations. Furthermore, 85% of MI measurements are within 1 standard deviation, which is 5% and 15% better than UWB and WiFi measurements respectively. This experiment confirms the advantage of MI measurements in the aspect of temporal stability.

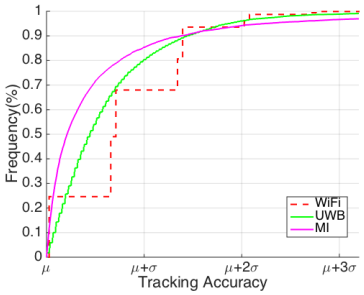

(a) Temporal Robustness

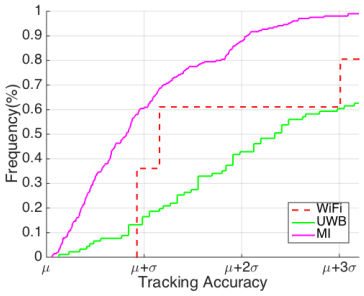

(b) Robustness to Moving People

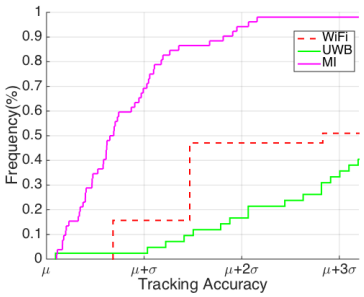

(c) Robustness to Moving Furniture

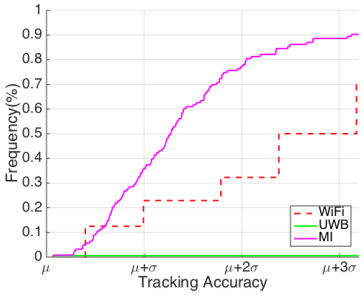

(d) Robustness to Various Heights

Fig. 7. Experiment 1: Comparison between MI, WiFi and UWB to environmental distortions.

Experiment 1(b) Robustness to Moving People: It is unavoidable that people work around in the motivating application scenarios, such as construction work, emergency response, etc. Therefore, it is important to choose a type of wireless signal for localisation that is robust to moving people. In

this experiment, we use the same deployment as Experiment 1(a), but one person walks across the line-of-the-sight between transmitters and receivers several times. Figure 7(a) shows the CDF of standard deviations of these three types of signals. For the MI signal, nearly 100% of the measurements are still within 3 standard deviations. However, the performance of WiFi and UWB drop dramatically. Only 80% and 62% of WiFi and UWB measurements respectively are within 3 standard deviations. Furthermore, 88% and 60% of MI measurements are within 2 and 1 standard deviations, which performs 27% and 23% better than WiFi measurements respectively, and more than 40% better than UWB measurements in both aspects. This again confirms the fact that the MI signal can penetrate the people thanks to the low carrier frequency and demonstrates its feasibility for our motivating application scenarios. By contrast, interference to UWB and WiFi caused by moving people unfortunately raises critical issues when these two type of signals are used as spatial features in localisation systems.

Experiment 1(c) Robustness to Moving Objects: Additional to the robustness to moving people, another important requirement for the use of spatial features for loop closure detection methods is the robustness to moving objects. We also use the same deployment as Experiment 1(a) but move an office chair between the-line-of-sight multiple times. Figure 7(c) shows the performance of these three signals. 98% , 95% and 69% of MI observations changes within 3, 2 and 1 standard deviations, respectively, which outperforms WiFi and UWB measurements significantly. Only 51% of WiFi measurements and 36% of UWB measurements vary within 3 standard deviations, 48% of WiFi measurements and 18% of UWB measurements vary within 2 standard deviations, and 17% of WiFi measurements and 2% of UWB measurements vary within 1 standard deviation.

Experiment 1(d) Robustness to Various Deployed Heights: Because we consider 2D localisation when designing the system, spatial features need to be robust to various heights. In this experiment, we deploy the receivers in the same location as Experiment 1(a), but in three different heights, i.e. 0 m, 0.5 m and 1 m. Figure 7(d) shows the CDF of standard deviations of these three types of wireless signals. 90% of MI measurements are within 3 standard deviations, and 76% and 36% of MI measurement vary within 2 and 1 standard deviations respectively. Using WiFi receivers in different heights, the percentages of the variations within 3, 2 and 1 standard deviations are 70%, 32% and 12%, respectively, which is not as stable as MI measurements. In terms of UWB, a significant variation occurs with changing heights, because UWB devices measure distance using time of flight. The deployment of the receivers in different heights results in massively different UWB measurements. This also confirms that a pair of UWB devices is not feasible for a localisation system and instead multiple devices need to be deployed in around the perimeter of the area, with good geometry.

C. Experiment 2: Loop Closure Robustness

The goal of this experiment is to evaluate the robustness of MI observations to determine loop-closure points. The path includes numerous repeated MI observations that will lead to a large number of loop closures as shown in Figure 8(a). During this experiment, the monitored person is walking in a square, which leads a 233.13 m path.

TABLE I
LOCALISATION ERROR OF EXPERIMENT 2

Method	IMU	MI	iMag	iMag+
e_{rms} (m)	4.527	4.247	0.752	0.752

Figure 8(b), Figure 8(c) and Figure 8(d) demonstrate the IMU, MI and iMag trajectories. Figure 8(e) shows the recovered trajectory after using the iMag+ method, which is virtually identical to the ground-truth and has corrected the odometry drift.

Table I shows that the e_{RMS} of IMU, MI, iMag and iMag+ methods are 4.527 m, 4.247 m, 0.752m and 0.752 m, respectively. Fusing measurements from MI and IMU, iMag+ can achieve 83.4% and 82.3% improvement compared with only using IMU and MI methods. Because the monitored person only walks in one quadrant in the coordinate system of the MI transmitter [7] in the experiment, the performances of iMag and iMag+ are the same. Figure 8(f) shows the CDF of errors using different methods. The results show that the 90th percentile localisation errors for IMU, MI and iMag+ are 7.24 m, 5.88 m and 1.129 m. In this metric, iMag+ achieves 84.4% and 80% improvements compared with the IMU and MI methods.

D. Experiment 3: Random Walking

The goal of this experiment is to show the performance of our proposed method with a more realistic motion trace. This ground truth of this experiment is shown in Figure 9(a). The monitored person walks randomly, which leads to a 311.95 m path.

Figure 9(b), Figure 9(c) and Figure 9(d) demonstrate the IMU, MI and iMag trajectories. Figure 9(e) shows the trajectory using iMag+ method. Table II shows that the e_{RMS} of IMU, MI, iMag and iMag+ method are 3.498 m, 4.564 m, 2.456 m and 1.908 m respectively. Fusing measurements from MI and IMU, it can achieve 45.5%, 58.2%, 22.3% improvements compared with IMU, MI and iMag based localisation methods. Figure 9(f) shows the CDF of errors using different methods. The results show that the 90th percentile localisation errors for IMU, MI, iMag and iMag+ methods are 4.9 m, 6.8 m, 4.0 m and 3.3 m. With this metric, iMag+ achieves 32.7%, 51.5% and 17.5% improvements compared with the IMU, MI and iMag methods.

This experiment demonstrates that even with long trajectories and sparse loop-closure points, iMag+ can accurately track users.

E. Experiment 4: Indoor Environment

In this section, we conduct experiments in a multi-storey build to show the performance of our proposed methods in

[7]The coordinate system of the MI transmitter is different from that in figures which show the performances of MI only methods. Those figures use the coordinates system of the ground truth recorded by the RTK GPS or Tango.

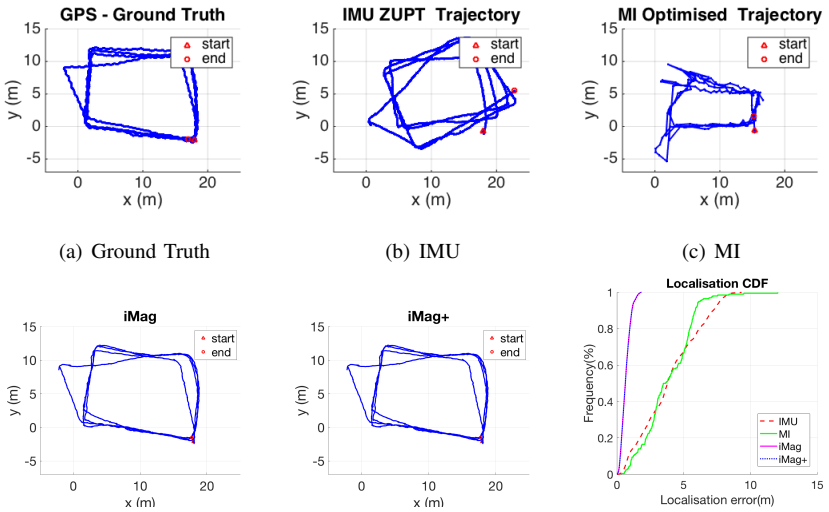

(a) Ground Truth (b) IMU (c) MI

(d) iMag (e) iMag+ (f) cdf

Fig. 8. Experiment 2: Trajectories and CDF of walking in a regular path in an open outdoor environment

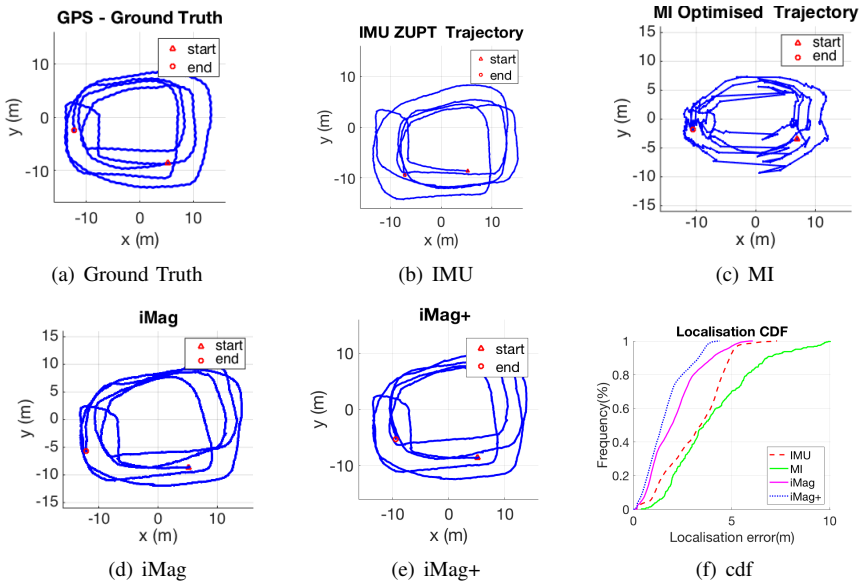

(a) Ground Truth (b) IMU (c) MI

(d) iMag (e) iMag+ (f) cdf

Fig. 9. Experiment 3: Trajectories and CDF for random walking

TABLE II
LOCALISATION ERROR OF EXPERIMENT 3

Method	IMU	MI	iMag	iMag+
e_{rms} (m)	3.4981	4.564	2.4562	1.9075

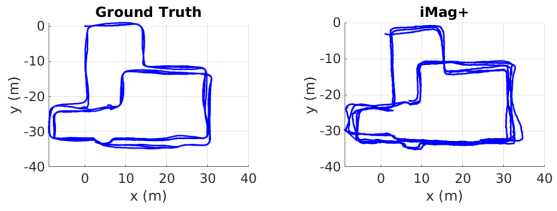

(a) Ground Truth (b) iMag+

Fig. 10. Experiment 4: Trajectories and CDF for indoor localisation.

indoor environments. Figure 10(a) and Figure 10(b) show the ground truth and trajectory on two floors obtained from our proposed method iMag+. Since our proposed method aims for 2D localisation, we will discuss the localisation results on two floors in the following sections respectively. We perform this experiment to show the feasibility and efficacy of our proposed cross-point loop closure method using MI observations in an indoor environment. This experiment is conducted in a modern office building, where large quantities of reinforcing steel are within the building structure. This experiment also aims to show the ability to find unique MI spatial signatures in an indoor environment.

1) Experiment 4-1: Indoor environment 1: The MI transmitter is deployed on the same floor of the experiment space. We collect MI signals with the monitored person walking

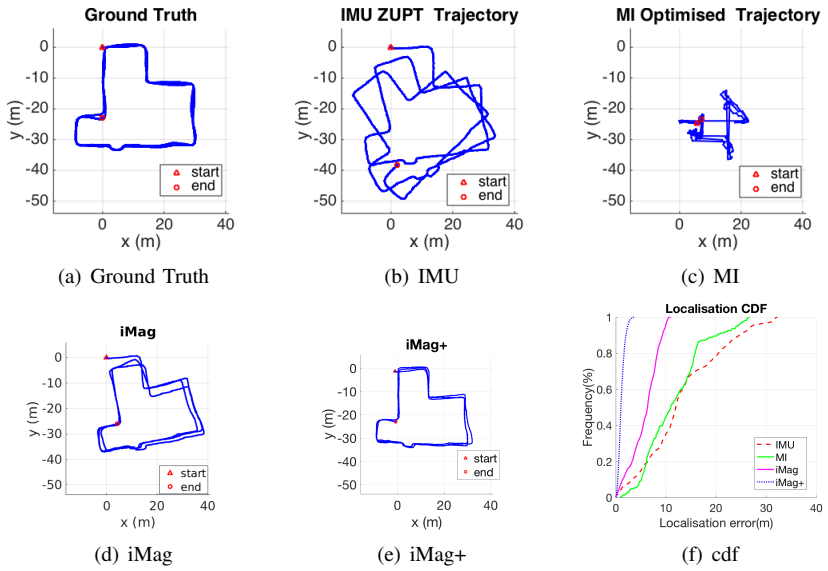

(a) Ground Truth (b) IMU (c) MI

(d) iMag (e) iMag+ (f) cdf

Fig. 11. Experiment 4: Trajectories and CDF for indoor localization.

TABLE III
LOCALISATION ERROR OF EXPERIMENT 4

Method	IMU	MI	iMag	iMag+
e_{rms} (m)	9.2635	8.9879	6.4332	1.2947

TABLE IV
LOCALISATION ERROR OF EXPERIMENT 5

Method	IMU	MI	iMag	iMag+
e_{rms} (m)	7.8838	24.8931	1.7768	1.3110

in this floor as shown in Figure 11(a). The path length is 390.77 m. When the user re-enters a previous place, the MI observations are correctly able to extract loop-closures, resulting in the corrected SLAM trajectory in Figure 11(e). There are multiple false negatives in the loop closure detection when using the loop closure method in the previously proposed iMag method, which cannot restore the trajectory correctly as shown in Figure 11(d). This indicates the importance of loop closure for localisation performance. Table III shows that the e_{RMS} of IMU, MI, iMag and iMag+ methods are 9.2635 m, 8.9879 m, 6.4332 m and 1.2947 m, respectively. Fusing measurement from MI and IMU, iMag+ can achieve 86.02%, 85.0%, 79.87% improvements compared with the IMU only, MI only and the iMag localisation method. Figure 11(f) shows the CDF of errors using different methods. The results show that the 90th percentile localisation errors for IMU, MI, iMag and iMag+ methods are 20.2 m, 24.6 m, 9.3 m and 2.2 m. In this metric, iMag+ achieves 89.11%, 91.06% and 76.34% improvements compared with the IMU, MI and iMag method.

This demonstrates that distorted MI observations are stable and unique in an indoor environment with metal structure, and have excellent discriminative power for loop-closure with the usage of our proposed first quadrant estimator.

2) Experiment 4-2: Indoor environment 2: The MI transmitter is left in the same location as Experiment 4-1, but the user walks one floor below the one where the MI transmitter is deployed as shown in Figure 12(a).

The corrected SLAM trajectory is shown in Figure 12(e). The path length is 333.17 m in this experiment. Table IV shows that the e_{RMS} of IMU, MI, iMag and iMag+ methods are 7.8838 m, 24.8931 m, 1.7768 m and 1.3110 m, respectively. Fusing measurement from MI and IMU, iMag+ can achieve 83.37%, 94.73%, 26.22% improvement compared with the IMU-based, MI-based and iMag localisation method.

Figure 11(f) shows the CDF of errors using MI only, IMU only and iMag, and iMag+. The results show that the 90th percentile localisation errors for IMU, MI, iMag and iMag+ methods are 10.3 m, 14.6 m, 2.7 m and 1.9 m. In this metric, iMag+ achieves 81.55%, 86.99%, 29.63% improvements compared with the IMU, MI and iMag methods.

As introduced, the resultant trajectory in this experiment along with that in Experiment 4-1 is derived using robust SLAM optimiser together to show the potential of localisation in the multi-storey building. This experiment demonstrates that our systems can be rapidly deployed and localise the user in a multi-storey building with only one transmitter. Note that our method assumes planar (2-D) motion, but level changes can easily be detected by using accelerometer data (e.g. stairs/elevator detection) or additional sensors, e.g. barometer, to make iMag+ function as a 2.5D location system.

F. Summary of Evaluation

Extensive evaluations show our proposed iMag+ is able to improve the localisation performance significantly. Due to the fact that only one MI transmitter is required, the deployment is very rapid. The localisation accuracy can achieve the localisation accuracy within no more than 1.9 m. The safety distance for big moving machinery is more than 2 m[45]. Therefore, our proposed method is sufficiently accurate for our motivating scenarios.

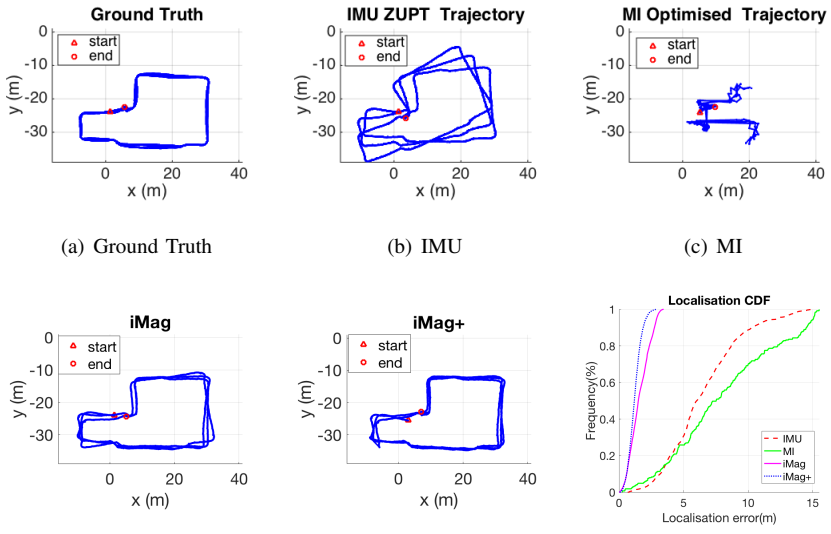

(a) Ground Truth (b) IMU (c) MI

(d) iMag (e) iMag+ (f) cdf

Fig. 12. Experiment 5: Trajectories and CDF for indoor localization. Note that the transmitter was placed on a different floor to the user, demonstrating the ability of MI to penetrate through solid concrete.

VI. Conclusions

In this paper, we proposed the iMag+ SLAM system and investigated its performance to meet the requirements of accurate localisation and rapid setup in both outdoor and indoor environments. A novel method of using low-frequency magneto-inductive based positioning coupled with inertial measurements demonstrates excellent accuracy, irrespective of the operating environment. Our prototype only needs one MI transmitter deployed in the area of interest, which allows for fast and easy setup, without any survey or calibration. Our evaluations show that our proposed method can achieve up to 90% improvement compared with using only an IMU or MI device for localisation. It is capable of operating equivalently well both indoor and outdoor environments.

Acknowledgment

This work was supported by Innovate UK Tracksafe (Project 102033) and in part by the NIST under Grant 70NANB17H185 and by UKRI under ACE-OPS EP/S030832/1.

References

[1] K. Lorincz, D. J. Malan, T. R. Fulford-Jones, A. Nawoj, A. Clavel, V. Shnayder, G. Mainland, M. Welsh, and S. Moulton, "Sensor networks for emergency response: challenges and opportunities," *Pervasive Computing, IEEE*, vol. 3, no. 4, pp. 16–23, 2004.

[2] Z. Xiao, H. Wen, A. Markham, and N. Trigoni, *Lightweight map matching for indoor localisation using conditional random fields*, 2014.

[3] L. Klingbeil and T. Wark, "A wireless sensor network for real-time indoor localisation and motion monitoring," in *Information Processing in Sensor Networks, 2008. IPSN'08. International Conference on*. IEEE, 2008, pp. 39–50.

[4] S. Papaioannou, H. Wen, Z. Xiao, A. Markham, and N. Trigoni, "Accurate Positioning via Cross-Modality Training," in *Proceedings of the 13th ACM Conference on Embedded Networked Sensor Systems - SenSys '15*. New York, New York, USA: ACM Press, 2015, pp. 239–251. [Online]. Available: http://dl.acm.org/citation.cfm?doid=2809695.2809712

[5] "Rail Safety and Standards Board Annual Safety Performance Report 2013/14," http://www.rssb.co.uk/Library/risk-analysis-and-safety-reporting/2014-07-aspr-2013-14-full-report.pdf, accessed: 2016-03-29.

[6] "Rail Safety and Standards Board Annual Safety Performance Report 2014/15," http://www.rssb.co.uk/Library/risk-analysis-and-safety-reporting/2015-07-aspr-full-report-2014-15.pdf, accessed: 2016-03-29.

[7] D. Bouvet and G. Garcia, "Improving the accuracy of dynamic localization systems using RTK GPS by identifying the GPS latency," in *2000 IEEE International Conference on Robotics and Automation.*, vol. 3. IEEE, pp. 2525–2530. [Online]. Available: http://ieeexplore.ieee.org/lpdocs/epic03/wrapper.htm?arnumber=846408

[8] "A Laser-Aided Inertial Navigation System (L-INS) for human localization in unknown indoor environments," *Proceedings - IEEE International Conference on Robotics and Automation*, pp. 5376–5382, 2010.

[9] E. S. Jones and S. Soatto, "Visual-inertial navigation, mapping and localization: A scalable real-time causal approach," *The International Journal of Robotics Research*, jan 2011. [Online]. Available: http://ijr.sagepub.com/cgi/doi/10.1177/0278364910388963

[10] G. Bellusci, D. Roetenberg, F. Dijkstra, H. Luinge, and P. Slycke, "Xsens MVN MotionGrid : Drift-free human motion tracking using tightly coupled ultra-wideband and miniature inertial sensors," *Xsens Technologies White Paper*, pp. 1–10, 2011.

[11] "Autoprowa Warning System," http://www.zoellner.de/en/, accessed: 2016-03-29.

[12] "ALARP Track Warining Project," http://www.transport-research.info/project/railway-automatic-track-warning-system-based-distributed-personal-mobile-terminals, accessed: 2016-03-29.

[13] "GPS Accuracy," http://www.gps.gov/systems/gps/performance/accuracy/, accessed: 2016-04-05.

[14] T. Takasu and A. Yasuda, "Development of the low-cost RTK-GPS receiver with an open source program package RTKLIB," *International symposium on GPS/GNSS*, 2009. [Online]. Available: http://gpspp.sakura.ne.jp/paper2005/isgps{_}2009{_}rklib.pdf

[15] R. P. Feynman, R. B. Leighton, and M. Sands, *The feynman lectures on physics*. American Journal of Physics, 1965.

[16] T. E. Abrudan, Z. Xiao, A. Markham, and N. Trigoni, "Distortion Rejecting Magneto-Inductive Three-Dimensional Localization (MagLoc)," *IEEE Journal on Selected Areas in Communications*, vol. 33, no. 11, pp. 2404–2417, 2015.

[17] B. Wei, N. Trigoni, and A. Markham, "imag: Accurate and rapidly deployable inertial magneto-inductive localisation," in *2018 IEEE International Conference on Robotics and Automation (ICRA)*. IEEE, 2018, pp. 99–106.

[18] X. Jiang, C.-J. M. Liang, K. Chen, B. Zhang, J. Hsu, J. Liu, B. Cao, and F. Zhao, *Design and evaluation of a wireless magnetic-based proximity detection platform for indoor applications*. New York, New York, USA: ACM, Apr. 2012.

[19] A. Markham, N. Trigoni, S. a. Ellwood, and D. W. Macdonald, "Revealing the hidden lives of underground animals using magneto-inductive tracking," *Proceedings of the 8th ACM Conference on Embedded Networked Sensor Systems - SenSys '10*, no. September, p. 281, 2010. [Online]. Available: http://portal.acm.org/citation.cfm?doid=1869983.1870011

[20] V. Pasku, A. De Angelis, M. Dionigi, G. De Angelis, A. Moschitta, and P. Carbone, "A Positioning System Based on Low Frequency Magnetic Fields," *IEEE Transactions on Industrial Electronics*, vol. 0046, 2015. [Online]. Available: http://ieeexplore.ieee.org/lpdocs/epic03/wrapper.htm?arnumber=7323819

[21] G. Pirkl and P. Lukowicz, "Robust, low cost indoor positioning using magnetic resonant coupling," in *Proceedings of the 2012 ACM Conference on Ubiquitous Computing - UbiComp '12*. New York, New York, USA: ACM Press, 2012, p. 431. [Online]. Available: http://dl.acm.org/citation.cfm?doid=2370216.2370281

[22] J. Sojdehei, P. Wrathall, and D. Dinn, "Magneto-inductive (MI) communications," in *MTS/IEEE Oceans 2001. An Ocean Odyssey. Conference Proceedings (IEEE Cat. No.01CH37295)*, vol. 1. Marine Technol. Soc, pp. 513–519. [Online]. Available: http://ieeexplore.ieee.org/lpdocs/epic03/wrapper.htm?arnumber=968775

[23] I. F. Akyildiz and E. P. Stuntebeck, "Wireless underground sensor networks: Research challenges," *Ad Hoc Networks*, vol. 4, no. 6, pp. 669–686, 2006.

[24] A. Markham and N. Trigoni, "Magneto-Inductive NEtworked Rescue System (MINERS): Taking sensor networks underground," *2012 ACM/IEEE 11th International Conference on Information Processing in Sensor Networks (IPSN)*, pp. 1–11, 2012. [Online]. Available: http://ieeexplore.ieee.org/lpdocs/epic03/wrapper.htm?arnumber=6920946

[25] S. A. Meybodi, J. Nielsen, J. Bendtsen, and M. Dohler, "Magneto-Inductive Underground Communications in a District Heating System," in *2011 IEEE International Conference on Communications (ICC)*. IEEE, jun 2011, pp. 1–5. [Online]. Available: http://ieeexplore.ieee.org/lpdocs/epic03/wrapper.htm?arnumber=5963067

[26] F. Evennou and F. Marx, "Advanced Integration of WiFi and Inertial Navigation Systems for Indoor Mobile Positioning," *EURASIP Journal on Advances in Signal Processing*, vol. 2006, pp. 1–12, 2006. [Online]. Available: http://asp.eurasipjournals.com/content/2006/1/086706

[27] B. Ferris, D. Fox, and N. Lawrence, "WiFi-SLAM using Gaussian process latent variable models," pp. 2480–2485, 2007.

[28] J. Huang, D. Millman, M. Quigley, D. Stavens, S. Thrun, and A. Aggarwal, "Efficient, generalized indoor WiFi GraphSLAM," *Proceedings - IEEE International Conference on Robotics and Automation*, pp. 1038–1043, 2011.

[29] H. Wang, A. Elgohary, and R. R. Choudhury, "No Need to War-Drive : Unsupervised Indoor Localization," *Proceedings of the 10th international conference on Mobile systems, applications, and services (MobiSys '12)*, pp. 197–210, 2012.

[30] Chao Gao and R. Harle, "Sequence-based magnetic loop closures for automated signal surveying," in *2015 International Conference on Indoor Positioning and Indoor Navigation (IPIN)*. IEEE, oct 2015, pp. 1–12. [Online]. Available: http://ieeexplore.ieee.org/lpdocs/epic03/wrapper.htm?arnumber=7346765

[31] P. Mirowski, T. K. Ho, Saehoon Yi, and M. MacDonald, "SignalSLAM: Simultaneous localization and mapping with mixed WiFi, Bluetooth, LTE and magnetic signals," in *International Conference on Indoor Positioning and Indoor Navigation*. IEEE, oct 2013, pp. 1–10. [Online]. Available: http://ieeexplore.ieee.org/lpdocs/epic03/wrapper.htm?arnumber=6817853

[32] J. Jung, T. Oh, and H. Myung, "Magnetic field constraints and sequence-based matching for indoor pose graph slam," *Robotics and Autonomous Systems*, vol. 70, pp. 92–105, 2015.

[33] I. Vallivaara, J. Haverinen, A. Kemppainen, and J. Röning, "Simultaneous localization and mapping using ambient magnetic field," in *Multisensor Fusion and Integration for Intelligent Systems (MFI), 2010 IEEE Conference on*. IEEE, 2010, pp. 14–19.

[34] D. Roetenberg, H. Luinge, and P. Slycke, "Xsens mvn: full 6dof human motion tracking using miniature inertial sensors," *Xsens Motion Technologies BV, Tech. Rep*, 2009.

[35] A. R. Jimenez, F. Seco, J. C. Prieto, and J. Guevara, "Indoor Pedestrian navigation using an INS/EKF framework for yaw drift reduction and a foot-mounted IMU," *Proceedings of the 2010 7th Workshop on Positioning, Navigation and Communication, WPNC'10*, pp. 135–143, 2010.

[36] G. Grisetti, R. Kümmerle, C. Stachniss, U. Frese, and C. Hertzberg, "Hierarchical optimization on manifolds for online 2d and 3d mapping," in *2010 IEEE International Conference on Robotics and Automation*. IEEE, 2010, pp. 273–278.

[37] C. Hertzberg, R. Wagner, U. Frese, and L. SchröDer, "Integrating generic sensor fusion algorithms with sound state representations through encapsulation of manifolds," *Inf. Fusion*, vol. 14, no. 1, pp. 57–77, Jan. 2013. [Online]. Available: http://dx.doi.org/10.1016/j.inffus.2011.08.003

[38] P. Agarwal, G. D. Tipaldi, L. Spinello, C. Stachniss, and W. Burgard, "Robust map optimization using dynamic covariance scaling," in *2013 IEEE International Conference on Robotics and Automation*. Citeseer, 2013, pp. 62–69.

[39] "Fast and Robust Curve Intersections," http://www.mathworks.com/matlabcentral/fileexchange/11837-fast-and-robust-curve-intersections/all_files, accessed: 2016-03-29.

[40] R. Kummerle, G. Grisetti, H. Strasdat, K. Konolige, and W. Burgard, "G2o: A general framework for graph optimization," in *2011 IEEE International Conference on Robotics and Automation*. IEEE, may 2011, pp. 3607–3613. [Online]. Available: http://ieeexplore.ieee.org/lpdocs/epic03/wrapper.htm?arnumber=5979949

[41] S. Thrun and M. Montemerlo, "The GraphSLAM algorithm with applications to large-scale mapping of urban structures," *International Journal on Robotics Research*, vol. 25, no. 5/6, pp. 403–430, 2005.

[42] "Google Tango Project," https://get.google.com/tango/, accessed: 2016-09-07.

[43] "Xsens MTi 1-series module," https://www.xsens.com/products/mti-1-series/, accessed: 2016-03-29.

[44] "Dacawave TREK1000 Evaluation Kit," https://www.decawave.com/product/trek1000-evaluation-kit/, accessed: 2019-10-23.

[45] "Safeguarding Machinery and Equipment," ehs.oregonstate.edu, accessed: 2019-10-23.

Bo Wei has been a senior lecturer in the Department of Computer and Information Sciences at Northumbria University. He was a lecturer and then a senior lecturer in Computer Science at Teesside University. Before joining Teesside, he was a Post-doctoral research assistant in University of Oxford. He obtained his PhD degree in Computer Science and Engineering in 2015 from the University of New South Wales, Australia. His research interests are Mobile Computing, Internet of Things, and Wireless Sensor Networks.

Niki Trigoni is Professor at the Oxford Department of Computer Science, heading the Cyber Physical Systems Group. Her interests lie in localisation and coordination of people and robots in GPS-denied environments using a variety of sensor modalities, including inertial, visual, magnetic and radio signals. She has applied her work to a number of application scenarios, including asset monitoring for construction sites, mobile autonomy with humans and robots, and track worker localisation for safety and efficiency. Trigoni is also Founder of the Navenio Oxford spinout.

Andrew Markham is an associate professor in the Department of Computer Science, at the University of Oxford. He received his BSc (Hons)(2004) and PhD(2008) both from the University of Cape Town, South Africa. He is a member of the cyber physical systems group and works in a number of interdisciplinary areas such as wildlife tracking, earthquake monitoring and industrial safety. Current research interests include data driven techniques for positioning, scene reconstruction and sensor processing.